

## Muon decay spectrum: leading logarithmic approximation

Andrej Arbuzov,\* Andrzej Czarnecki,† and Andrei Gaponenko‡  
*Department of Physics, University of Alberta Edmonton, AB T6G 2J1, Canada*

$\mathcal{O}(\alpha^2 \ln^2(m_\mu/m_e))$  QED corrections to the electron spectrum and angular distribution in muon decay are evaluated. Impact on the determination of Michel parameters is estimated. Current theoretical uncertainty in the muon decay distributions is discussed.

PACS numbers: 13.35.Bv, 14.60.Ef, 12.20.Ds

### I. INTRODUCTION

The decay  $\mu^+ \rightarrow e^+ \nu_e \bar{\nu}_\mu$  has been very accurately studied. Its total rate determines the Fermi constant  $G_\mu$  describing the strength of the weak interactions [1]. Standard Model predicts other features of this decay, such as the positron energy and angular distribution, positron polarization, and a variety of correlations between spins and momenta of the muon and its decay products [2, 3, 4, 5]. Precise determinations of those observables test the Standard Model and can be used to search for possible “new physics” effects [6]. This motivates ongoing studies of the positron transverse [7] and longitudinal polarization [8] and angular/energy distributions [9, 10]. Muon lifetime is also being remeasured [11, 12].

Current experiments are so precise that theoretical predictions must include radiative corrections beyond the first order in the fine structure constant  $\alpha \simeq 1/137.036$ . For the muon lifetime they are known [13, 14, 15, 16, 17, 18, 19] through  $\mathcal{O}(\alpha^2)$ . On the other hand, little is known about the positron energy distribution beyond the  $\mathcal{O}(\alpha)$  effects [16, 20].

The experiment TWIST at Canada’s National Laboratory TRIUMF is designed to measure the positron spectrum from polarized  $\mu^+$  decays with a precision of  $10^{-4}$  [9, 10]. To match this, and help search for “new physics” effects, the Standard Model prediction must include at least the leading  $\mathcal{O}(\alpha^2)$  effects in the positron distribution.

We have examined the dominant effects at this order, which arise due to emission of collinear photons and  $e^+e^-$  pairs. Such effects do not significantly affect the total muon lifetime, but they rearrange the positron spectrum. They are enhanced by two powers of the muon and electron mass ratio logarithm  $L \equiv \ln(m_\mu^2/m_e^2) \simeq 10.66$  (this roughly determines their order of magnitude,  $(\alpha^2/\pi^2)L^2 \simeq 6 \cdot 10^{-4}$ ).

We are interested in the energy and angular distribution of positrons produced in the  $\mu^+$  decay. We normalize it so that it coincides with the differential width of the decay in the two lowest orders in  $\alpha$ . A difference occurs at  $\mathcal{O}(\alpha^2)$  where an additional positron can appear due to pair production. The differential distribution of positrons (summed over  $e^+$  spin states) in the polarized muon decay is

$$\frac{d^2 N^{\mu^+ \rightarrow e^+ \nu \bar{\nu}}}{dz d \cos \theta} = \Gamma_0 [F(z) - \cos \theta P_\mu G(z)], \quad \Gamma_0 \equiv \frac{G_\mu^2 m_\mu^5}{192 \pi^3} \left( 1 + \frac{3}{5} \frac{m_\mu^2}{m_W^2} \right),$$

$$z \equiv \frac{2E}{(1+r^2)m_\mu}, \quad r \equiv \frac{m_e}{m_\mu}, \quad z_0 \leq z \leq 1, \quad z_0 \equiv \frac{2r}{1+r^2}, \quad (1)$$

where  $m_e$  and  $m_\mu$  are the electron and muon masses;  $\theta$  is the angle between the positron flight direction and the muon spin (for the  $\mu^-$  decay, the sign of the  $\cos \theta$  term should be reversed);  $P_\mu$  is the degree of the muon polarization;  $E$  is the positron energy.

Functions  $F(z)$  and  $G(z)$  describe the isotropic and anisotropic parts of the positron spectrum. They can be expanded in series in  $\alpha$ ,

$$F(z) = f_{\text{Born}}(z) + \frac{\alpha}{2\pi} f_1(z) + \left( \frac{\alpha}{2\pi} \right)^2 f_2(z) + \mathcal{O}(\alpha^3), \quad (2)$$

\*Electronic address: aarbuzov@phys.ualberta.ca

†Electronic address: czar@phys.ualberta.ca

‡Electronic address: agapon@phys.ualberta.ca

and similarly for  $G(z)$ .

To match the precision of TWIST, the electron mass should be included at the Born level,

$$\begin{aligned} f_{\text{Born}}(z) &= 6(1+r^2)^4 v z \left[ z(1-z) + \frac{2}{9} \rho (4z^2 - 3z - z_0^2) + \eta z_0 (1-z) \right], \\ g_{\text{Born}}(z) &= -2(1+r^2)^4 v^2 z^2 \xi \left[ 1-z + \frac{2}{3} \delta (4z - 3 - r z_0) \right], \\ v &\equiv \sqrt{1 - \frac{m_e^2}{E^2}}, \end{aligned} \quad (3)$$

where  $\rho$ ,  $\eta$ ,  $\xi$ , and  $\delta$  are the so-called Michel parameters [21, 22, 23] which depend on the Lorentz structure of the interaction responsible for the decay. In this paper we assume that the decay is caused by the Standard Model  $V - A$  interaction, for which  $\rho = 3/4$ ,  $\eta = 0$ ,  $\xi = 1$ , and  $\delta = 3/4$ . These values agree with present experimental fits [24],

$$\begin{aligned} \rho &= 0.7518 \pm 0.0026, \\ \eta &= -0.007 \pm 0.013, \\ \xi P_\mu &= 1.0027 \pm 0.0079 \pm 0.0030, \\ \delta &= 0.7486 \pm 0.0026 \pm 0.0028. \end{aligned} \quad (4)$$

In the massless limit ( $m_e \rightarrow 0$ ) we have

$$f_{\text{Born}}(z) \rightarrow f_0(z) = z^2(3-2z), \quad g_{\text{Born}}(z) \rightarrow g_0(z) = z^2(1-2z). \quad (5)$$

Functions  $f_1$  [16] and  $g_1$  [20] are also known with full dependence on the electron mass. However, at present it is sufficient to use their massless limit given in the Appendix.

The  $\mathcal{O}(\alpha^2)$  effects are not yet known. They can be divided up into three parts according to the power of  $L$ ,

$$f_2(z) = \frac{(L-1)^2}{2} f_2^{\text{LL}}(z) + (L-1) f_2^{\text{NLL}}(z) + \Delta f_2(z), \quad (6)$$

and similarly for  $g_2$ . In this paper we evaluate the leading logarithmic (LL) corrections  $f_2^{\text{LL}}$  and  $g_2^{\text{LL}}$ . We divide them into contributions of pure photon emissions and of diagrams with  $e^+e^-$  pairs,

$$f_2^{\text{LL}} \equiv f_2^{\text{LL}(\gamma)} + f_2^{\text{LL}(e^+e^-)}, \quad g_2^{\text{LL}} \equiv g_2^{\text{LL}(\gamma)} + g_2^{\text{LL}(e^+e^-)}. \quad (7)$$

In diagrams with  $e^+e^-$  pairs we have to clarify the meaning of the variable  $z$ , whether it describes the energy of the ‘‘primary’’ positron or the one from the pair. (We can neglect interference in the LL approximation.) These two possibilities give rise to the so-called non-singlet (NS) and singlet (S) parts of pair corrections,

$$f_2^{\text{LL}(e^+e^-)} \equiv \frac{2}{3} f_{2\text{NS}}^{\text{LL}(e^+e^-)} + f_{2\text{S}}^{\text{LL}(e^+e^-)}, \quad g_2^{\text{LL}(e^+e^-)} \equiv \frac{2}{3} g_{2\text{NS}}^{\text{LL}(e^+e^-)} + g_{2\text{S}}^{\text{LL}(e^+e^-)}. \quad (8)$$

Ingredients needed to evaluate the full LL effect in eq. (7) are given below in eqs. (14, 15) (photonic corrections) and (18, 19) (pairs).

## II. LEADING LOGARITHMIC APPROXIMATION

The LL corrections can be found by convoluting the tree level spectrum (5) with the positron structure function (SF), a solution of the Dokshitzer–Gribov–Lipatov–Altarelli–Parisi evolution equations for QED. Analytical expressions for  $\mathcal{D}(w, \beta)$  are known [25, 26, 27] up to the fifth order in  $\alpha$  so that terms  $\mathcal{O}(\alpha^n L^n)$  can be found for  $n = 1, \dots, 5$  (in this paper we treat  $n \leq 2$ ).

To find the various corrections outlined in the Introduction, we divide the SF into three parts: pure photonic, and non-singlet (NS) and singlet (S)  $e^+e^-$  pair contributions,

$$\begin{aligned} \mathcal{D}(w, \beta) &\equiv \mathcal{D}_\gamma(w, \beta) + \mathcal{D}_{e^+e^-}^{\text{NS}}(w, \beta) + \mathcal{D}_{e^+e^-}^{\text{S}}(w, \beta), \\ \mathcal{D}_\gamma(w, \beta) &= \delta(1-w) + \sum_{n=1} \frac{\beta^n}{n!} P^{(n)}(w), \\ \mathcal{D}_{e^+e^-}^{\text{NS}}(w, \beta) &= \frac{\beta^2}{3} P^{(1)}(w) + \mathcal{O}(\alpha^3 L^3), \\ \mathcal{D}_{e^+e^-}^{\text{S}}(w, \beta) &= \frac{\beta^2}{2} R(w) + \mathcal{O}(\alpha^3 L^3), \quad \beta \equiv \frac{\alpha}{2\pi} (L-1). \end{aligned} \quad (9)$$

The components  $\mathcal{D}_\gamma$  and  $\mathcal{D}_{e^+e^-}^{\text{NS}}$  correspond to those Feynman diagrams in which the registered positron belongs to the same fermionic line as the initial one. If the registered positron arises from a pair production, its LL contribution to the energy spectrum is described by the singlet function  $\mathcal{D}_{e^+e^-}^{\text{S}}$ . Functions relevant for our work are

$$\begin{aligned}
P^{(n)}(w) &= \lim_{\Delta \rightarrow 0} \left[ P_\Delta^{(n)} \delta(1-w) + P_\Theta^{(n)} \Theta(1-w-\Delta) \right], \quad \Theta(w) = \begin{cases} 1 & \text{for } w \geq 0 \\ 0 & \text{for } w < 0 \end{cases}, \\
P_\Theta^{(1)}(w) &= \frac{1+w^2}{1-w}, \quad P_\Delta^{(1)} = 2 \ln \Delta + \frac{3}{2}, \\
P_\Theta^{(2)}(w) &= 2 \left[ \frac{1+w^2}{1-w} \left( 2 \ln(1-w) - \ln w + \frac{3}{2} \right) + \frac{1+w}{2} \ln w - 1 + w \right], \quad P_\Delta^{(2)} = \left( 2 \ln \Delta + \frac{3}{2} \right)^2 - \frac{2}{3} \pi^2, \\
R(w) &= \frac{1-w}{3w} (4 + 7w + 4w^2) + 2(1+w) \ln w.
\end{aligned} \tag{10}$$

Higher order expressions and further details on the SF formalism can be found in [25, 27, 28, 29, 30].

To find the LL corrections we use convolution, defined by

$$A(\bullet) \otimes B(z) = \int_0^1 dw \int_0^1 dw' \delta(z - ww') A(w) B(w') = \int_z^1 \frac{dw}{w} A(w) B\left(\frac{z}{w}\right). \tag{11}$$

For example, to reproduce the first order LL correction, we convolute the Born-level spectrum with  $P^{(1)}$ ,

$$f_1^{\text{LL}}(z) = P^{(1)}(\bullet) \otimes f_0(z) = \frac{5}{6} + 2z - 4z^2 + \frac{8}{3}z^3 + 2z^2(3-2z) \ln \frac{1-z}{z}, \tag{12}$$

$$g_1^{\text{LL}}(z) = -\frac{1}{6} - 4z^2 + \frac{8}{3}z^3 + 2z^2(1-2z) \ln \frac{1-z}{z}. \tag{13}$$

These formulas coincide with the LL parts of the full  $\mathcal{O}(\alpha)$  results given in the Appendix. A comparison of the LL and full first order functions is presented in Fig. 1. We see that the LL approximation gives the bulk of the  $\mathcal{O}(\alpha)$  correction, especially in the region of intermediate and large values of  $z$ , relevant for TWIST.

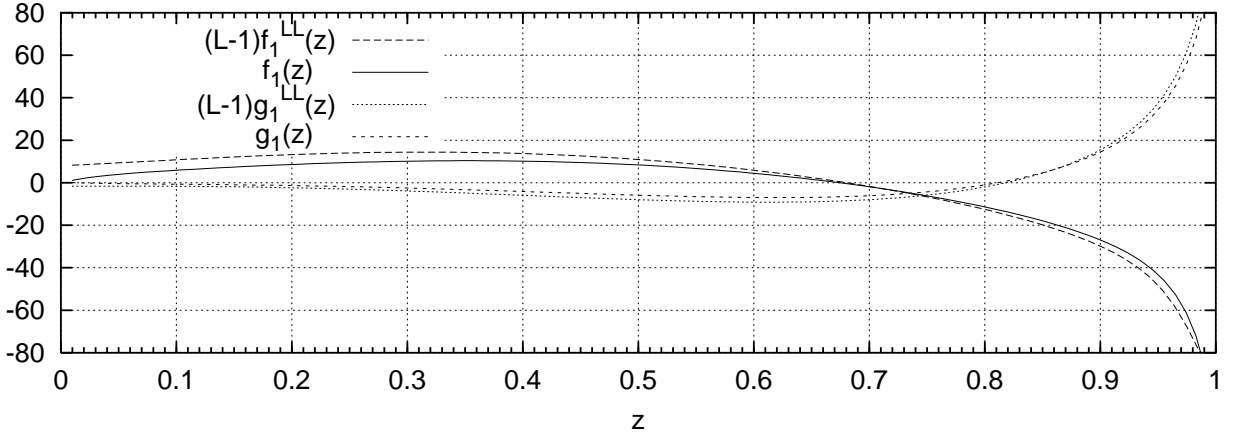


FIG. 1: Values of functions  $f_1$  and  $g_1$  versus  $z$ : exact results (eq. (A1)) and LL approximations (eqs. (12,13)).

For the second order photonic LL corrections, we convolute with  $P^{(2)}$ ,

$$\begin{aligned}
f_2^{\text{LL}(\gamma)}(z) &= P^{(2)}(\bullet) \otimes f_0(z) \\
&= 4z^2(3-2z)\Phi(z) + \left( \frac{10}{3} + 8z - 16z^2 + \frac{32}{3}z^3 \right) \ln(1-z) \\
&\quad + \left( -\frac{5}{6} - 2z + 8z^2 - \frac{32}{3}z^3 \right) \ln z + \frac{11}{36} + \frac{17}{6}z + \frac{8}{3}z^2 - \frac{32}{9}z^3, \\
g_2^{\text{LL}(\gamma)}(z) &= 4z^2(1-2z)\Phi(z) + \left( -\frac{2}{3} - 16z^2 + \frac{32}{3}z^3 \right) \ln(1-z)
\end{aligned} \tag{14}$$

$$\begin{aligned}
& + \left( \frac{1}{6} + 8z^2 - \frac{32}{3}z^3 \right) \ln z - \frac{7}{36} - \frac{7}{6}z + \frac{8}{3}z^2 - \frac{32}{9}z^3, \\
\Phi(z) \equiv \text{Li}_2 \left( -\frac{1-z}{z} \right) + \ln^2 \frac{1-z}{z} - \frac{\pi^2}{6}, \quad \text{Li}_2(z) \equiv - \int_0^z \frac{dy}{y} \ln(1-y).
\end{aligned} \tag{15}$$

In the same manner we can get the third order photonic contributions.

Integrals of the LL photonic contributions vanish,

$$\int_0^1 dz f_1^{\text{LL}}(z) = \int_0^1 dz f_2^{\text{LL}(\gamma)}(z) = \int_0^1 dz g_1^{\text{LL}}(z) = \int_0^1 dz g_2^{\text{LL}(\gamma)}(z) = 0, \tag{16}$$

in accord with the theorem about the cancellation of mass singularities [31, 32].

A numerical illustration of our results for the relative size of the second order LL photonic corrections is given in Fig. 2, where we plot the relative correction defined as

$$\delta_2^{\text{LL}(\gamma)} = \left( \frac{\alpha}{2\pi} \right)^2 \frac{(L-1)^2}{2} \left( \frac{f_2^{\text{LL}(\gamma)}(z) - \cos\theta g_2^{\text{LL}(\gamma)}(z)}{f_0(z) - \cos\theta g_0(z)} \right). \tag{17}$$

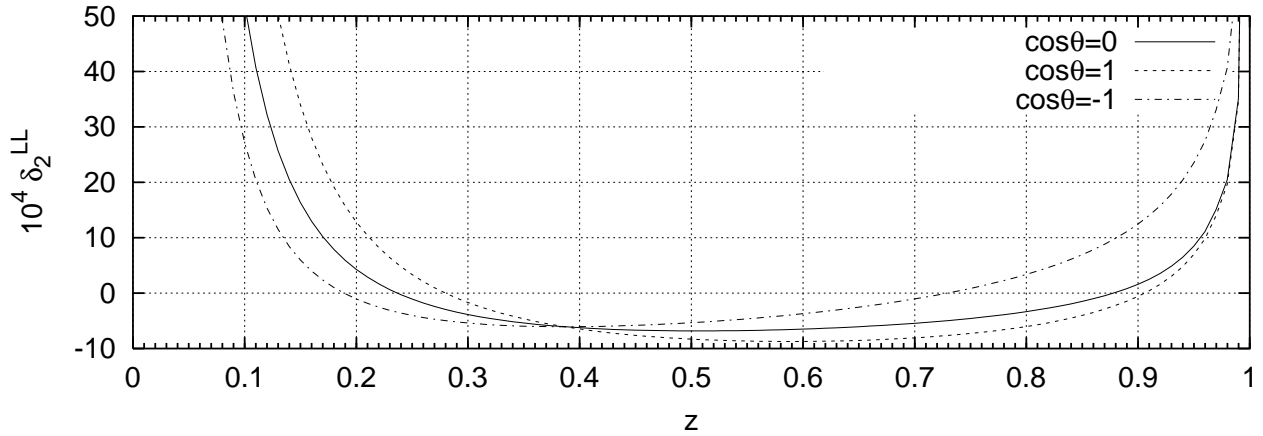


FIG. 2: Relative size of the second order LL photonic corrections for as a function of  $z$ , plotted for three values of  $\cos\theta$ .

In  $\mathcal{O}(\alpha^2)$  the positron distribution has a contribution from real and virtual  $e^+e^-$  pairs. Virtual effects of heavier fermions are negligible [37]. Pair corrections are found by convoluting  $f_0$  and  $g_0$  with  $P^{(1)}$  (non-singlet) and  $R$  (singlet),

$$f_{2\text{NS}}^{\text{LL}(e^+e^-)}(z) = f_1^{\text{LL}}(z), \quad g_{2\text{NS}}^{\text{LL}(e^+e^-)}(z) = g_1^{\text{LL}}(z) \quad (\text{see eqs. (12,13)}), \tag{18}$$

$$f_{2\text{S}}^{\text{LL}(e^+e^-)}(z) = \frac{17}{9} + \frac{2}{3z} + 3z - \frac{14}{3}z^2 - \frac{8}{9}z^3 + \left( \frac{5}{3} + 4z + 4z^2 \right) \ln z,$$

$$g_{2\text{S}}^{\text{LL}(e^+e^-)}(z) = -\frac{1}{9} - \frac{2}{9z} + z + \frac{2}{9}z^2 - \frac{8}{9}z^3 + \left( -\frac{1}{3} + \frac{4}{3}z^2 \right) \ln z. \tag{19}$$

In Table I, numerical results are presented for the quantity  $\delta_2^{\text{LL}(e^+e^-)}$ , which gives the relative size of the second order LL pair correction with respect to the Born distribution (for  $P_\mu = 1$ ),

$$\delta_2^{\text{LL}(e^+e^-)} = \int_{w_{\min}}^1 \frac{dw}{w} \frac{f_0(z/w) - \cos\theta g_0(z/w)}{f_0(z) - \cos\theta g_0(z)} \left[ \mathcal{D}_{e^+e^-}^{\text{NS}}(w, \beta) + \mathcal{D}_{e^+e^-}^{\text{S}}(w, \beta) \right], \quad w_{\min} = \max \left\{ z, \frac{z}{z+y} \right\}, \tag{20}$$

where  $y$  is the cut on the maximal energy fraction of the real pair,  $E_{\text{pair}} \leq ym_\mu/2$ . Both the singlet and the non-singlet pair contributions are taken into account. It means that we simulated the situation, where an observation of two positrons is treated as a pair of simultaneous  $\mu^+$  decays.

TABLE I: Leading logarithmic pair correction  $10^4 \delta_2^{\text{LL}(e^+e^-)}$  for  $\cos\theta = -1$ .

$z \backslash y$	0.1	0.2	0.3	0.4	0.5
0.05	5.60	20.62	51.01	99.44	164.88
0.1	1.90	5.15	10.03	16.83	25.32
0.2	0.46	1.66	2.83	4.07	5.35
0.3	-0.10	0.73	1.36	1.91	2.36
0.5	-0.72	-0.14	0.17	0.35	0.40
0.7	-1.18	-0.80	-0.71	-0.71	-0.71
0.9	-2.01	-2.01	-2.01	-2.01	-2.01

In general, effects due to  $e^+e^-$  pairs depend on experimental conditions and cuts for events with several charged particles in the final state.

If one is interested in the total LL effect due to real and virtual  $e^+e^-$  pairs to the muon decay width, one has to drop the singlet pair contributions  $f_{2S}^{\text{LL}(e^+e^-)}(z)$  and  $g_{2S}^{\text{LL}(e^+e^-)}(z)$ , to avoid double counting of real pairs. Cancellation of the leading logarithms in the total decay width is guaranteed by (16).

### III. EXPONENTIATION

Toward the energy spectrum end point ( $z \rightarrow 1$ ), the first order correction  $f_1^{\text{LL}}$  and  $g_1^{\text{LL}}$  diverge. This phenomenon, discussed in Refs. [16, 33], is a signal to look beyond the first order approximation. One can use the Yennie–Frautschi–Suura theorem [34] to re-sum the divergent terms and convert them into an exponential function. Exponentiated representations of the SF can be employed to re-sum parts of the leading logs to all orders in  $\alpha L$  [28, 35]. The exponentiation for the muon decay has been criticized [36], because the large logarithmic terms contain a mass singularity: not all large logs disappear in the terms supplied by the exponent after an integration over the energy, like in eq. (16).

As has been discussed in [2], the validity of exponentiation is limited to the region near the end of the spectrum. One can see from the  $\mathcal{O}(\alpha)$  results that the exponentiation can be relevant only in a very small range where  $z$  differs from 1 by about  $10^{-10}$  (the correction is about  $-50\%$  at  $1 - z = 10^{-10}$ ), which is much less than the experimental resolution. For this reason we leave our results in the un-exponentiated, fixed order form.

The end region of the spectrum is usually excluded from the fits of Michel parameters. This is done to reduce the uncertainty due to the finite energy resolution, which is most important in this region. Indeed, the shape of an experimentally observed spectrum is a convolution of the “true” spectrum with a resolution function. In the “bulk” part the effect of the finite resolution is very small. However near a sharp edge (with the width much less than the width of the resolution function) the shape of the convoluted spectrum is defined mainly by the resolution function and not by the spectrum. Exclusion of the end point region helps also to reduce the theoretical uncertainty because this is where the unknown higher-order corrections are expected to be the largest.

### IV. CONCLUSIONS

To estimate the effect of the second order correction on values of Michel parameters measured in an experiment, we generated a 2D distribution in  $z$  and  $\cos\theta$  according to the RC-corrected spectrum and fitted with a spectrum without the corrections.

$10^9$  toy Monte Carlo “events”  $\{z, \cos\theta\}$  were produced by sampling the 2-dimensional spectrum (1) taking into account the complete first order corrections and the second order LL photonic ones. This level of statistics is expected to be accumulated in the TWIST experiment [10]. The acceptance–rejection method and the Mersenne Twister random number generator [38] was used. Events passing the “acceptance cuts”  $0.34 \leq |\cos\theta| \leq 0.98$ ,  $0.4 \leq z$  and the cut  $z \leq z_{\text{max}}$  were filled into a 2D histogram.  $z_{\text{max}}$  varied between 0.96–0.995. The cuts roughly represented acceptance of the TWIST detector [10]. The region of  $z$  close to 1 was excluded to avoid the issue of the experimental resolution, discussed above. Finally, a maximum loglikelihood fit of the spectrum *without* the second order RC to the histogram was done.  $\rho$ ,  $\eta$ ,  $\xi$ ,  $\delta$ , and the global normalization were the 5 free parameters of the fit. We put  $P_\mu = 1$  both in the generation and in the fits. Binning of the histogram was chosen sufficiently fine, so that repeating the

procedure with several times smaller bins gave the same results. Self-consistency of the method was checked by fitting the histogram with the full spectrum. Original values of Michel parameters were reproduced within the errors.

We have observed statistically significant deviations of the fitted Michel parameters from their original values when doing the fits without the  $f_2^{\text{LL}(\gamma)}$  and  $g_2^{\text{LL}(\gamma)}$  contributions. That emphasizes the importance of using a precise enough theoretical spectrum shape for extracting values of Michel parameters in an experiment.

Shifts of Michel parameters due to radiative corrections depend on the fit region, and perhaps on other factors not considered here. For example, one may want to take into account the effect of the finite experimental resolution in the bulk part of the spectrum. Fig. 3 demonstrates dependence of the shifts on the upper energy limit of the fit region.

For a realistic value of the cut,  $z_{\text{max}} = 0.97$ , the shifts of Michel parameters due to the second order LL corrections are of the order

$$\begin{aligned}\Delta\rho &\simeq 11 \cdot 10^{-4}, \\ \Delta\eta &\simeq 350 \cdot 10^{-4}, \\ \Delta\xi &\simeq 3 \cdot 10^{-4}, \\ \Delta\delta &\simeq 4 \cdot 10^{-4}.\end{aligned}\tag{21}$$

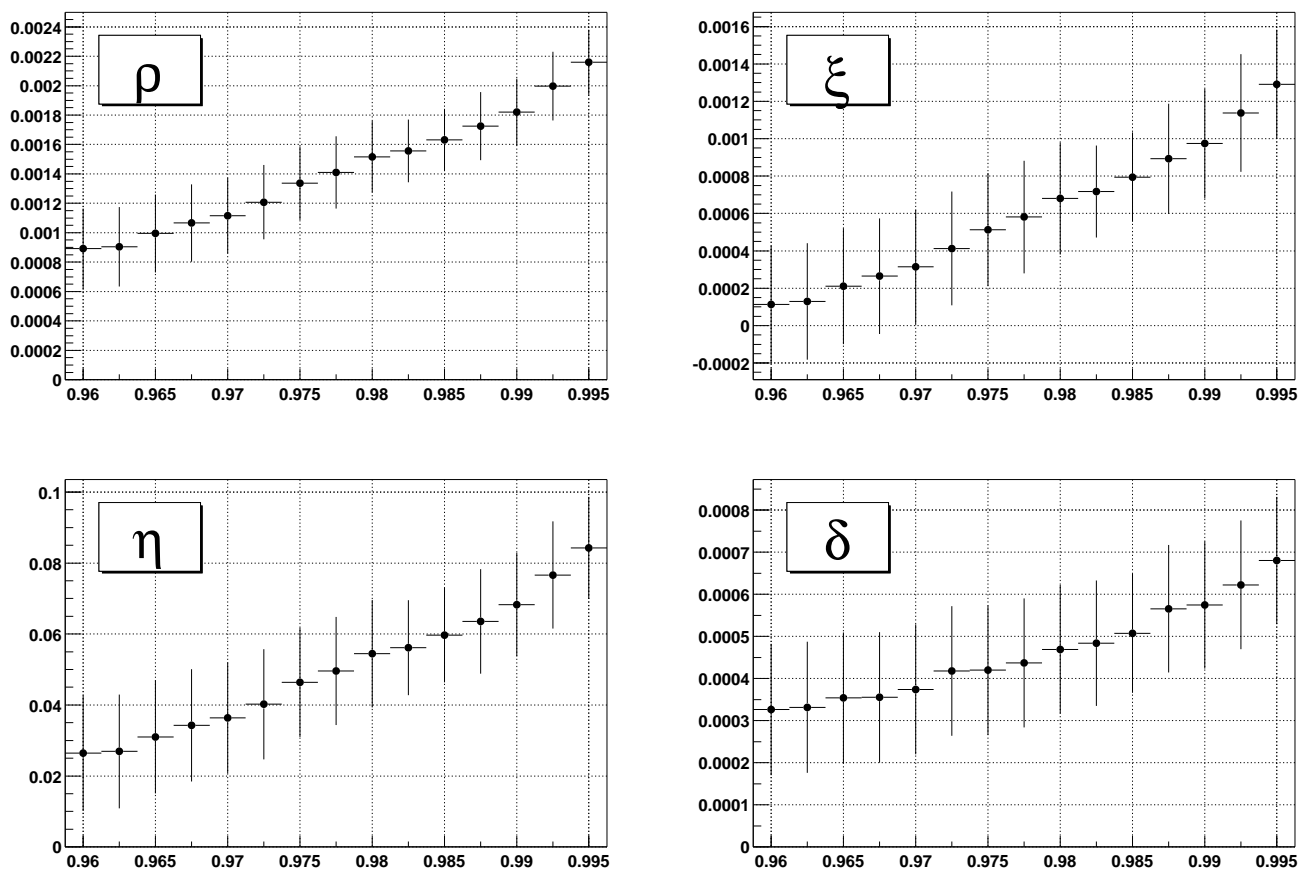


FIG. 3: Shifts of Michel parameters due to the second order radiative correction for different upper energy cuts. Horizontal axis is  $z_{\text{max}}$ , vertical axis is the difference between a reconstructed parameter and its Standard Model value. The points are correlated since they are obtained from the same data set.

The relatively large shift of  $\eta$  is due to the fact that it enters the spectrum with a small coefficient  $z_0 \simeq 10^{-2}$ . If we fix  $\eta$  during the fits to its SM value 0, the shifts due to  $\mathcal{O}(\alpha^2)$  effects become  $5 \cdot 10^{-4}$  for  $\rho$ ,  $-3 \cdot 10^{-4}$  for  $\xi$ , and  $3 \cdot 10^{-4}$  for  $\delta$ . Comparing the results for free and fixed  $\eta$  we observe a strong correlation of  $\eta$  with  $\rho$  and  $\xi$ .

Fig. 3 indicates a rather strong dependence of all Michel parameters on  $z_{\text{max}}$ . It follows from the peaked behavior of the radiative corrections when  $z$  is close to 1. The fitting procedure tries to compensate the effects of radiative corrections and cuts by adjusting Michel parameters and the global normalization.

The remaining theoretical uncertainty in the muon decay spectrum, eq. (1), is due to unknown contributions  $\mathcal{O}(\alpha^2 L)$  and  $\mathcal{O}(\alpha^n L^n)$ ,  $n \geq 3$ . Non-logarithmic terms of the order  $(\alpha/\pi)^2 \simeq 5.4 \cdot 10^{-6}$  are expected to be small (compared with the  $10^{-4}$  precision tag). The sub-leading contributions  $\mathcal{O}(\alpha^2 L)$  are the main source of the remaining uncertainty. The magnitude of the corresponding photonic contribution can be estimated using the known second order photonic LL correction,

$$\delta_2^{\text{NLL}(\gamma)} \sim \frac{3}{L} \delta_2^{\text{LL}(\gamma)} \simeq 0.3 \delta_2^{\text{LL}(\gamma)}, \quad (22)$$

where we multiplied by 3 to account for the unknown coefficient of sub-leading terms. The leading contributions from higher orders ( $n \geq 3$ ) can be estimated using again the second order LL result,

$$\delta_3^{\text{LL}(\gamma)} \sim 3 \frac{\alpha}{2\pi} L \delta_2^{\text{LL}(\gamma)} \simeq 0.03 \delta_2^{\text{LL}(\gamma)}. \quad (23)$$

$e^+e^-$  pair contributions are typically smaller than those of the photons, at least in the LL.

These estimates of unknown radiative corrections can be converted into theoretical uncertainties  $\sigma^{\text{th}}$  of Michel parameters, of the order of a third of the shifts in eq. (21) we found by including the LL photonic corrections. With  $z_{\text{max}} = 0.97$  we find

$$\begin{aligned} \sigma^{\text{th}}(\rho) &= 3 \cdot 10^{-4}, \\ \sigma^{\text{th}}(\eta) &= 100 \cdot 10^{-4}, \\ \sigma^{\text{th}}(\xi P_\mu) &= 1 \cdot 10^{-4}, \\ \sigma^{\text{th}}(\delta) &= 1 \cdot 10^{-4}. \end{aligned} \quad (24)$$

The conditions and the fitting procedure in a concrete experiment can be different from the ones described above. The actual size of the effect of radiative corrections on Michel parameters can be derived there in a similar way, starting from the analytical formulas for theoretical predictions and applying specific experimental conditions.

The planned accuracy of the TWIST experiment [9, 10] is

$$\begin{aligned} \sigma^{\text{exp}}(\rho) &= 1 \cdot 10^{-4}, \\ \sigma^{\text{exp}}(\eta) &= 30 \cdot 10^{-4}, \\ \sigma^{\text{exp}}(\xi P_\mu) &= 1.3 \cdot 10^{-4}, \\ \sigma^{\text{exp}}(\delta) &= 1.4 \cdot 10^{-4}. \end{aligned} \quad (25)$$

Clearly, effects of the second order LL radiative corrections, eq. (21), have to be taken into account at this level of accuracy. In order to further reduce the theoretical uncertainty, the next-to-leading second order corrections should be evaluated as well. Work on this is in progress.

### Acknowledgments

This research was supported by the Natural Sciences and Engineering Research Council of Canada, the Alberta Ingenuity Fund, and the University of Alberta. We thank Carl Gagliardi, Nathan Rodning, and Vladimir Selivanov for valuable discussions concerning experimental conditions and the fitting procedure. A.A. is grateful for the hospitality of the Brookhaven National Laboratory and TRIUMF.

\*

### APPENDIX A: FIRST ORDER CORRECTIONS

$\mathcal{O}(\alpha)$  corrections to the muon decay spectrum, without terms suppressed by  $m_e^2/m_\mu^2$ , read [16]

$$\begin{aligned} f_1(z) &= (L-1)f_1^{\text{LL}}(z) + 2z^2(3-2z)R_1(z) + \frac{1-z}{6} [(10+34z-32z^2)\ln z + 5-27z+34z^2], \\ g_1(z) &= (L-1)g_1^{\text{LL}}(z) + 2z^2(1-2z)R_1(z) - \frac{1+27z^2-16z^3}{3}\ln z - \frac{1-z}{6}(7-13z-30z^2) - \frac{4(1-z)^3}{3z}\ln(1-z), \\ R_1(z) &\equiv -2\text{Li}_2(1-z) + \ln z \ln(1-z) - 2\ln^2 z - \frac{\ln(1-z)}{z} - \frac{5}{4}. \end{aligned} \quad (A1)$$

$f_1^{\text{LL}}(z)$  and  $g_1^{\text{LL}}(z)$  are defined in eqs. (12,13).

- 
- [1] W. J. Marciano, Phys. Rev. **D60**, 093006 (1999), hep-ph/9903451.
  - [2] A. M. Sachs and A. Sirlin, in *Muon Physics*, edited by C. Wu and V. Hughes (Academic Press, New York, 1977), vol. 2, p. 49.
  - [3] F. Scheck, Phys. Rept. **44**, 187 (1978).
  - [4] W. Fetscher, H. J. Gerber, and K. F. Johnson, Phys. Lett. **B173**, 102 (1986).
  - [5] W. Fetscher and H. J. Gerber, in *Precision tests of the standard electroweak model*, edited by P. Langacker (World Scientific, Singapore, 1995), p. 657.
  - [6] Y. Kuno and Y. Okada, Rev. Mod. Phys. **73**, 151 (2001), hep-ph/9909265.
  - [7] K. Bodek et al., AIP Conf. Proc. **539**, 167 (2000).
  - [8] R. Prieels et al., in *Intersections of particle and nuclear physics*, edited by Z. Parsa and W. J. Marciano (AIP, Melville, NY, 2000), p. 920.
  - [9] N. L. Rodning et al., Nucl. Phys. Proc. Suppl. **98**, 247 (2001).
  - [10] M. Quraan et al., Nucl. Phys. **A663**, 903 (2000).
  - [11] R. Carey and D. Hertzog et al., PSI Proposal.
  - [12] J. Kirkby et al., PSI Proposal (May 1999).
  - [13] S. Berman and A. Sirlin, Ann. Phys. **20**, 20 (1962).
  - [14] R. E. Behrends, R. J. Finkelstein, and A. Sirlin, Phys. Rev. **101**, 866 (1956).
  - [15] S. M. Berman, Phys. Rev. **112**, 267 (1958).
  - [16] T. Kinoshita and A. Sirlin, Phys. Rev. **113**, 1652 (1959).
  - [17] T. van Ritbergen and R. G. Stuart, Phys. Rev. Lett. **82**, 488 (1999), hep-ph/9808283.
  - [18] M. Steinhauser and T. Seidensticker, Phys. Lett. **B467**, 271 (1999), hep-ph/9909436.
  - [19] A. Czarnecki and K. Melnikov (2001), hep-ph/0112264.
  - [20] A. B. Arbuzov, Phys. Lett. **B524**, 99 (2002), hep-ph/0110047.
  - [21] L. Michel, Proc. Phys. Soc. **A63**, 514 (1950).
  - [22] C. Bouchiat and L. Michel, Phys. Rev. **106**, 170 (1957).
  - [23] T. Kinoshita and A. Sirlin, Phys. Rev. **108**, 844 (1957).
  - [24] D. E. Groom *et al.* (*Particle Data Group*), Eur. Phys. J. **C15**, 1 (2000).
  - [25] M. Skrzypek, Acta Phys. Polon. **B23**, 135 (1992).
  - [26] M. Przybycień, Acta Phys. Polon. **B24**, 1105 (1993), hep-th/9511029.
  - [27] A. B. Arbuzov, Phys. Lett. **B470**, 252 (1999), hep-ph/9908361.
  - [28] E. A. Kuraev and V. S. Fadin, Sov. J. Nucl. Phys. **41**, 466 (1985), [Yad. Fiz. **41**, 733 (1985)].
  - [29] O. Nicrosini and L. Trentadue, Phys. Lett. **B196**, 551 (1987).
  - [30] E. A. Kuraev, JETP Lett. **65**, 127 (1997), hep-ph/9611294.
  - [31] T. Kinoshita, J. Math. Phys. **3**, 650 (1962).
  - [32] T. D. Lee and M. Nauenberg, Phys. Rev. **133**, 1549 (1964).
  - [33] W. J. Marciano, G. C. Marques, and N. Papanicolaou, Nucl. Phys. **B96**, 237 (1975).
  - [34] D. R. Yennie, S. C. Frautschi, and H. Suura, Ann. Phys. **13**, 379 (1961).
  - [35] M. Cacciari, A. Deandrea, G. Montagna, and O. Nicrosini, Europhys. Lett. **17**, 123 (1992).
  - [36] M. Roos and A. Sirlin, Nucl. Phys. **B29**, 296 (1971).
  - [37] A. I. Davydychev, K. Schilcher, and H. Spiesberger, Eur. Phys. J. **C19**, 99 (2001), hep-ph/0011221.
  - [38] M. Matsumoto and T. Nishimura, ACM Transactions on Modeling and Computer Simulation **8**, 3 (1998), see also [www.math.keio.ac.jp/~matumoto/emt.html](http://www.math.keio.ac.jp/~matumoto/emt.html).